Assessment of Soil Erosion Potential in Semi-Arid Soils Using Hyperspectral Technology

E. Ben-Dor,[1,4] N. Goldshalager,[2] O. Braun,[3] B. Kindel,[4] A.F.H. Goetz,[4] D. Bonfil,[5] M. Agassi,[2] Y. Binyaminy,[2] and A. Karnieli[6]

[1]Department of Geography and Human Environment, Tel-Aviv University, Israel
[2]Soil Erosion Research Station, Soil Conservation and Drainage Division, Ministry of Agriculture, Israel
[3]Bar-Kal Systems Engineering, Ltd., Netania, Israel
[4]Center for the Study of Earth from Space, Cooperative Institute for Research in Environment Sciences (CIRES), University of Colorado, Boulder, Colorado
[5]Gilat Experimental Station, Ministry of Agriculture, Israel
[6]The Remote Sensing Laboratory, Jacob Blaustein Institute for Desert Research, Ben Gurion University of the Negev, Israel

INTRODUCTION

Soil erosion by water runoff is a matter of great concern in both bare and agricultural lands. This process may lead to significant effects, such as water lost to the soil profile, decline in soil fertility and productivity, and increased peak stream flow, as well as associated floods. The main cause of the runoff from rain and overhead irrigation water is the structural crust that develops over bare soils during rainfall or irrigation events that significantly reduces the soils' infiltration rate. The hydraulic conductivity of this crust is a few orders of magnitude lower than that of the underlying soil (e.g., McIntyre, 1958; Morin and Benyamini, 1977). Whenever the hydraulic conductivity of the crust is lower than the rainfall intensity, ponding, runoff and soil erosion will occur.

Most of the available methods for assessing the physical crust status use disturbed soil samples that do not represent exact field conditions (Keren and Singer, 1989, 1991) or use simulation techniques that cannot mirror exact field conditions (Agassi and Bradford, 1999). Consequently, mapping and predicting soil structural crust processes are of great interest and importance to soil scientists and farmers. Apparently, crust potential mapping is not a straightforward problem, and to the best of our knowledge, this technique has never been conducted.

Recent studies by Goldshalager et al. (2001, 2002) and Ben-Dor et al. (2003), showed significant relationship existed between selected wavelengths readings and infiltration rates, when measured under controlled laboratory conditions. Further, they were able to create a spectral library that contains spectra of three soils from Israel, in varying rain energies and crust position, and to show that a different correlation existed for each soil.

Because significant spectral changes occur within the soil surface as a result of raindrop impact (see Goldshalager et al., 2002), it is assumed that the hyperspectral technology will enable capturing of spatial variation within a rain-affected field and will provide a real-time spatial overview of soil crust related properties (such as soil erosion and infiltration). The purpose of this study is to examine the feasibility of hyperspectral technology together with careful

laboratory and field measurements in order to identify soil properties that are related to the structural crust formation and status over agricultural soils in Israel.

MATERIALS AND METHODS

The area selected for this study is located in the Negev area of southern Israel in the fields of the Experimental Farm Station of Gilat. The soils in this area are Loamy Loess and defined as Loess by the local Israeli definition system (Dan and Raz, 1970) and calcic haploxeralf according to the USDA definition (Soil Survey Staff, 1975). The mechanical composition is 28% clay, 47% silt and 25% sand and the mineralogy of the soil, estimated by XRD is: ~14% montmorillonite, ~50% kaolinite, ~27% illite and ~17% calcite. The area is relatively dry, having annual precipitation of about 200 mm concentrated mostly during December through April.

The Flight Campaign

The airborne sensor selected for this study is the Airborne Image Spectrometer for Applications (AISA) (Mäkisara et al., 1993). The AISA is a programmed computable push broom airborne imaging spectrometer with wavelength range between 400 and 900 nm. The size of the CCD detector array is 384 by 286 pixels and the spectral bandwidth is >1.5 nm (max. 186 channels) which can be summed up to 9.6 nm. The swath width is 384 pixels and the IFOV is 1 mrad, enabling a pixel size of 1 meter from 1000 meter altitude where the FOV is 22°. The integration (exposure) time is 4 ms, and the pixel data is digitized to 12 bits. On March 24, 2001, the AISA sensor was mounted onboard a twin engine piper Aztec aircraft and flown over the study area in altitude of 3000 meter (providing about 3 meter pixel size and 1.2 km swath) with 30 spectral bands (421–888 nm) characterized by Full Width Half Max (FWHM) ranging from 1.55 to 1.71 nm. The signal-to-noise ratio of the sensor over a 50% albedo target provides reasonable values ranging around a value of 90 (maximum 125 minimum 20). The raw data was radiometerically converted into radiance using laboratory calibration file provided by the SpecIm© company which were collected prior to the flight. The radiance data were corrected into reflectance units using an ACORN code (Atmospheric CoRrection Now, ACORN, 2001) polished by ground reflectance spectra of 4 soil samples that were taken during the overpass on the ground.

Laboratory Study

Rain Simulator

Soils were collected from a nearby field, brought to the laboratory, air-dried and then, passed through a 4-mm sieve. Two experiments (several months apart) using two batches of soils were employed to determine the relationship between the spectroscopy and the infiltration rate of the soil in the laboratory. The soils in each experiment were identically packed into 30 x 50-cm perforated soil boxes, 4 cm deep, over a layer of 6 cm coarse sand. Four runs (two for each experiment) were employed. For each run, the boxes were placed on a soil box carousel, 5 boxes per run, at a 5% slope, and were subjected to a simulated rainstorm, using distilled water (Morin et al., 1967). In each experiment, at first run, the simulated rainstorm provided a fog type rain (no energy), having intensity similar to the infiltration rate of the soil. The storm lasted until the measured rate of percolation (in this case also infiltration) reached that of the measured simulated rainstorm intensity. Then the rainfall was stopped and the soil boxes were left to rest until drainage ceased from all the boxes. One soil box was randomly taken out and photographed. At this stage the rainfall energy was changed to ~22.3 joule mm^{-1} m^{-2}. The carousel was rotated again with four of the remaining soil boxes, which were subjected to

rainstorm intensity approximately similar to the initial infiltration rates of the soil. At first the storm lasted until ~3.5 mm of rainfall had been applied (equal to ~70–80 joule) during which time the infiltration rate was continuously measured. Then one box was randomly removed and photographed. This procedure was repeated several times until ~89 mm of rainfall was accumulated (see Table 1 for more details). After the rainstorm was stopped, the soil boxes were oven-dried for 48 h. at 35°C and then for a week at room temperature. In Table 1 also given are the equivalent infiltration rate measured for each rainstorm event, the accumulated rain amount and its corresponding energy are presented. Fifteen to twenty soil samples were taken from each box for spectral reflectance measurements in the laboratory without disturbing the soil crust. These measurements were carried out, using ASD spectrometer with a portable light source that measured a soil sample under a constant halogen illumination and reflectance geometry conditions across the VIS-NIR-SWIR region (0.4–2.4 μm). The reflectance of the soil samples was measured against Halon, and the final spectrum of each measurement was presented relative to this reference. An average spectrum for every rain treatment was calculated, using the samples taken from each soil box. The spectra were stored and later processed to analyze the spectral-infiltration relationship. In several locations around the study areas, samples were collected from the surface (the upper 1 cm), covering an area of about 5 m^2, brought to the laboratory and analyzed for $CaCO_3$.

Table 1: Infiltration rate and rain storm energy for each treatment used in the crust simulator experiment.

Accumulated Rain Energy (Joule)	Infiltration Rate (mm/Joule)	Rain Accumulation (mm)
0	44	0
0	48	0
71	32	3.2
80	37	3.6
109	28.5	4.9
145	24	6.5
160	35	7.1
216	21	9.7
280	30	12.5
290	17	13
400	25	17.8
506	11.5	22.7
560	17.5	25
613	11.5	27.5
800	12	35.6
1012	7	45.4
1270	7	57
1842	3.5	82.6
1985	4.6	89

Field Measurements

During the overpass, soil samples were collected around the area from several targets to enable rectifying the radiometric measurements into relative reflectance. Four controlling soil plots, within the agricultural areas field of Gilat farm, were selected to study the crust spectral response

from the air. The plots were characterized by a noticeable crust that formed during rainstorm events that lasted two months (100 mm). Each plot was divided into two subplots: 1) the "non crust" plot, composed of bare soil, with the thin crust broken by a gentle plowing of the upper soil layer 24 hours before the flight, and 2) "crusted" plot, composed of crust soils (formed by natural rain) with noticeable crust occurrences. The last rain event in the area (affecting the "crusted" plots) was reported in March 10, 2001 (2 mm) suggesting that the soil maintained a basic hygroscopic moisture capacity which was measured to be around 4%.

Results and Discussion

Figure 1 provides a gray scale subset image that sampled from the entire flight line image and covers the study area. Also overlain in this image are selected controlled plots and the exact locations of the soil sampling for the $CaCO_3$ determination. The study area is rather flat, characterized with vegetation (beans, barely and wheat) side by side to the bare soil plots (with and without organic residual). The soil plots are marked on the image (1–4) to draw the attention for further discussion. From looking on the image it is noticeable, that albedo variation occurred within these selected plots (1-4) as well as within other areas along the image. One of the basic factors that control soil brightness in an arid environment is the $CaCO_3$ content. Basically, this component can be assessed from hyperspectral technology, simply by using the strong absorption feature at 2330 nm (Gaffey, 1986). However, as the AISA sensor does not cover the SWIR region, this information cannot be extracted from the current data base and hence cannot confirm or reject the above brightness assumption. To check this, we used the 18 soil samples (randomly sampled) and their $CaCO_3$ content measured in the laboratory. Plotting the $CaCO_3$ content versus the albedo parameter of each ground target (calculated from the area under the spectral curve between 489 to 888 nm) shows no correlation between the two (Figure 2). This suggests that the albedo tone variation may have emerged from another source and probably from the physical crust formation.

Figure 3 presents a ground overview of one of the field plot (Plot-3 in Figure 1) after breaking the soil crust with a discus (non-crusted) at 24 hours before the flight, whereas some small-crusted areas can be visible at the edge of this plot. The photo also shows a close Nadir view from 80 cm. It is evident that by naked eyes, a soil color changes from bright to dark tones is visible within the soils based on their crusting position.

Extracting the spectra of each plot (calculated from an average of about 40 pixels) showed that the spectral base line (and hence the soil albedo) is higher in the crusted soils than in the non-crusted soils. Figure 4 provided the spectral reflectance of the selected plots, with and without the crust layer. The crust plots are higher in about 3-6% (reflectance units) or about 30% (in relative values) than the non crusted plots.

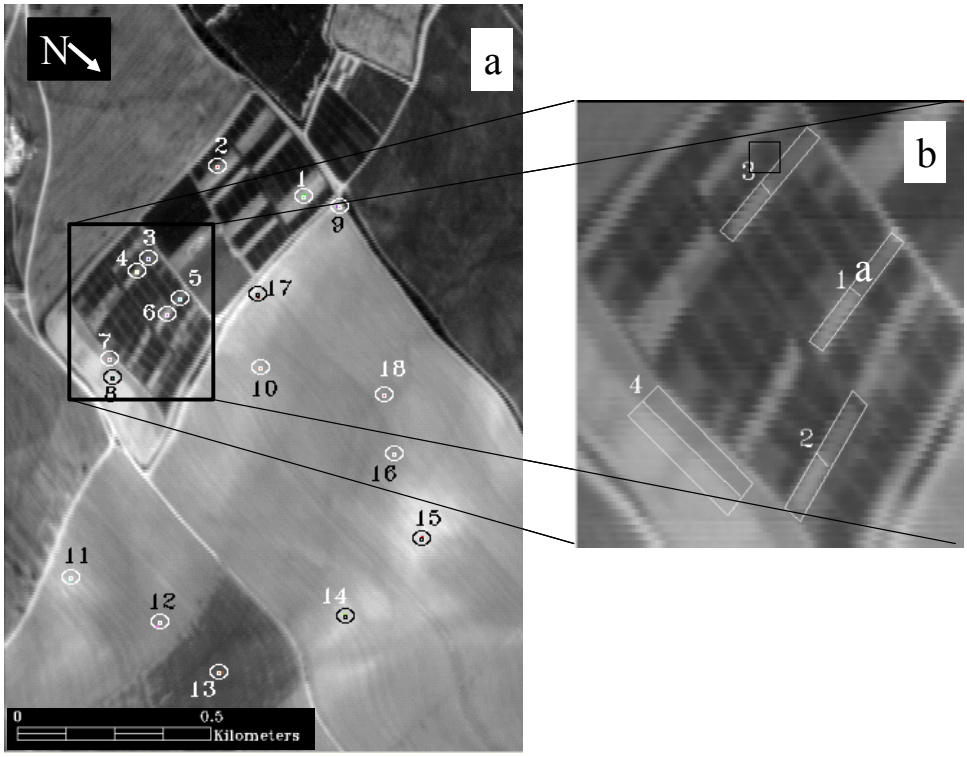

Figure 1: The study area on a grayscale image (band 14, 576 nm): (a) the position of the controlled plots (crusted and non-crusted) and (b) the ground soil sample (for $CaCO_3$ content analysis) overlain.

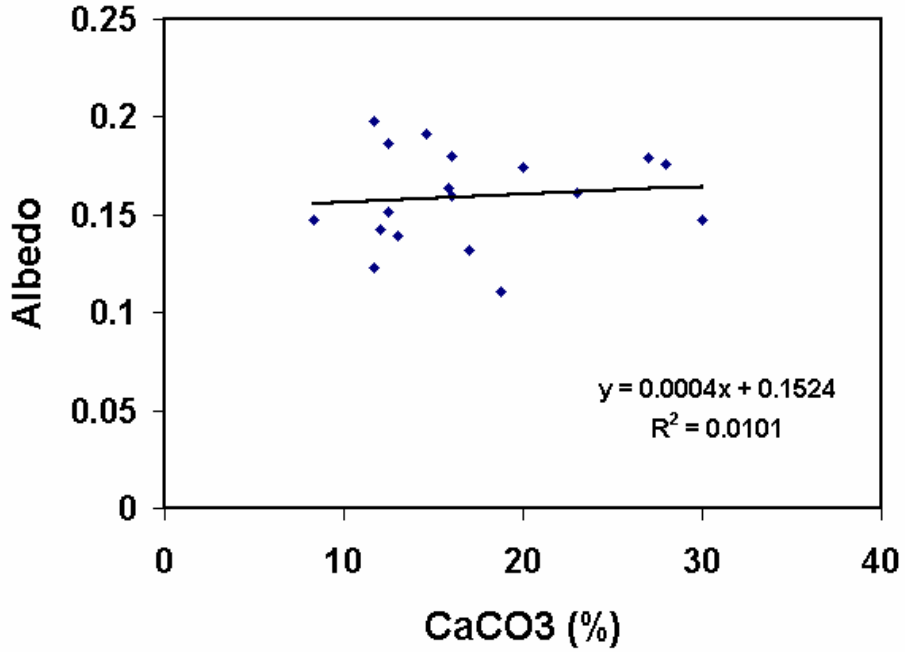

Figure 2: The relationship between the $CaCO_3$ content versus the albedo (the area under the spectral curve between 489 to 888 nm) of the samples shown in Figure 3.

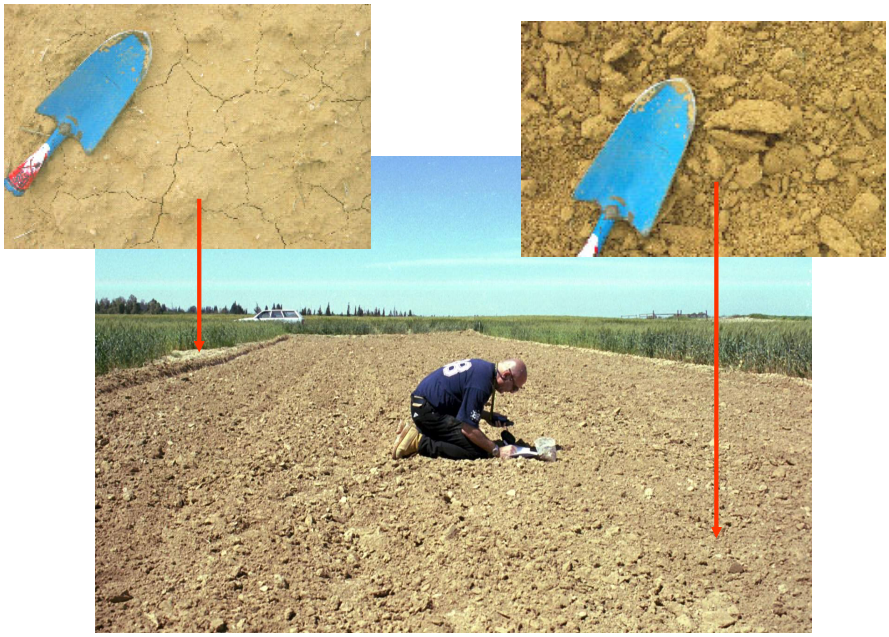

Figure 3: An overview image of Plot 3 in its discus position (non-crusted). Also provided are two enlargement images showing the crusted (a) and non-crusted (b) soils from a distance of 80 cm.

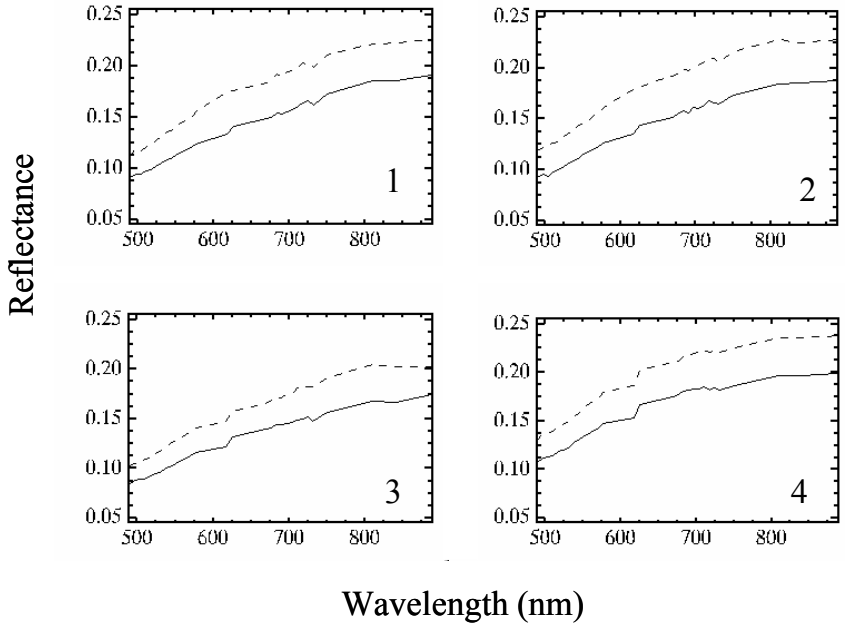

Figure 4: The reflectance spectra of the controlled plots in both crusted and non-crusted position. Dot lines represent the crusted soil (light tones in Figure 1) and solid line the non-crusted soil (dark tones in Figure 1).

Figure 5 provides an overview of the soil in the laboratory tray after applying rainstorm at energies of 613 and 1842 joule/m^2 (taken from the first experiment). Also presented is the bulk soil with no rain energy (non-crusted soil). It is well observed from this figure that albedo changes occur in the direction just as observed in the field: in the high raindrop energy—the soil

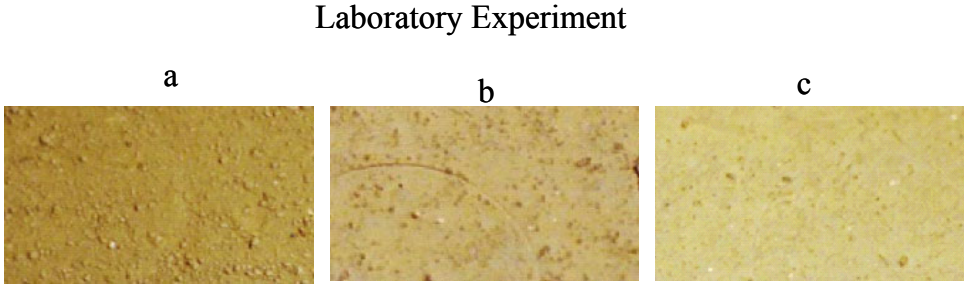

Figure 5: Three images showing the crust position after the rain simulator treatments in three different rain energies: (a) 0, (b) 613 joule m^2, and (c)1842 joule m^2.

are brighter, whereas in the low (or no) raindrop energy—the soils are darker. The spectra of all treatments are given in Figure 6 (a,b). As well seen, a noticeable spectral sequence occurs, going from a low raindrop energy (low crusted) to a high raindrop energy (highly crusted) rain. These values are equivalent to high and low infiltration rates respectively, as measured simultaneously during the rainstorm event and are given in Table 1. The overall reflectance changes in the laboratory were found to be similar to what were found in the image: 3% in the lower energies and 8% in the highest energies levels. As seen, the shape of the spectra is constant with rain energy (no new spectral features or slope changes occurs when going from one rain energy to another) where the only significant spectral change is the reflectance offset. It is interesting to note that Goldshalager et al., 2001 have found that in the SWIR region, not only albedo changes are noticeable, but also changes in the spectral features positions and intensity occurs. This is based mainly on the specific spectral information of OH in clay minerals across the SWIR region, which is not active in the current AISA VIS-NIR spectral region.

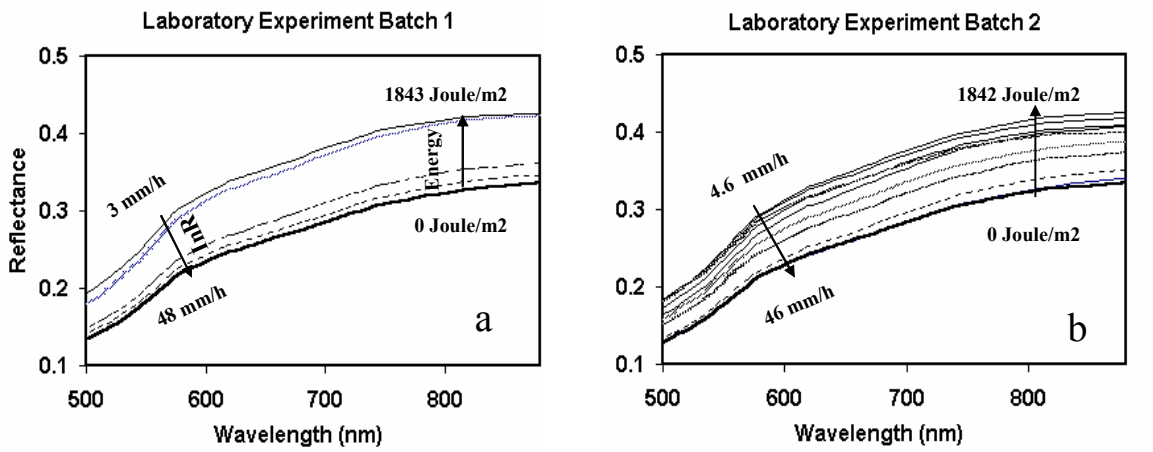

Figure 6: The laboratory spectra of the crusted soil after applying different rain energies to the soils (a represent the first experiment and b represent the second experiment taken in few months apart).

Although the VIS region is less informative than the SWIR region, the albedo changes observed in the laboratory treatments suggest that quantitative relationship between spectral parameters and the crusting phenomenon may be possible. To quanitively assess this relationship, we calculated the Normalized Spectral Area (NSA), which is the area under the ratio curve (generated by using a crusted soil (test) spectrum against standard non crusted soil spectrum

(reference)). The ratio spectra are given Figure 7(a,b) and show that the ratio spectra increased as the rain energy increased and the infiltration rate decreased. Plotting the area under the ratio curve (NSA) against the infiltration rates is given in Figure 8. A significant relationship between the two parameters (infiltration rate versus the NSA) was obtained (r2= 0.83). In order to apply the NSA model to the field data, the reflectance image data were processed as the laboratory spectral data. In this regard, we selected a polygon from a selected "non-crusted" sub plot of plot-3 (see Figure 1) and used it as a reference in which every pixel in question may be calculated for its NSA. In order to apply the calibration equation obtained in the laboratory for the entire area, all non-soil pixels were masked out and then the model was applied on a (soil) pixel by pixel basis. The result is an image given in Figure 9 with a color ramp representing the "Infiltration Rate" (InR) values. In the processed image, several areas holding high and low InR values can be seen. The low InR area (marked as A on the image) is a plowed (dry) field, which exhibits NSA values within the detection limit of the InR calibration curve. Based on the NSA values of this soil, it is assumed that the current plot is holding a good (non) crust condition in which the soil infiltration potential is high and the erosion risk is minimal. The high InR areas (marked as B, C and D) are holding InR values that are outside the calibration range. Area B represents a dirt road enriched with high $CaCO_3$ content (27%) lime which is relatively higher than the average $CaCO_3$ content of the entire population that stands on 13.8% (SD 5%). Area C also consists of high $CaCO_3$ content (30%) and thus are not suspected to be crusted under the current analysis where area D consists of $CaCO_3$ content of 14.6%; and hence represents a significant crusted area. Another factor inherent in the calibration results is the soil moisture status (wet or dry) that also can change the soil color tones. This parameter can as well as the $CaCO_3$ features can be masked out by using the SWIR region, and hence by AVIRIS, but not with the current AISA sensor. More study in this direction has to be applied to make the crust mapping more accurate and totally independent of field information. Using the AVIRIS sensor in this direction, may be a step forward to achieve this aim. The spectral information suggests that there is a significant potential to do so under more complex soils systems.

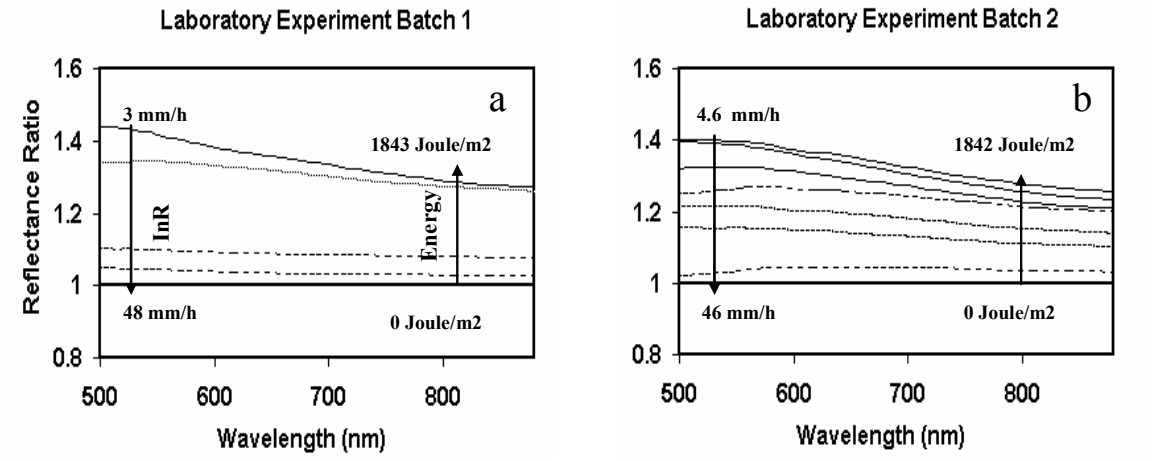

Figure 7: The ratio spectra of the laboratory treatment shown in Figure 8. Each spectrum composed of the reflectance at every rain energy treatment against the reflectance at 0 energy level.

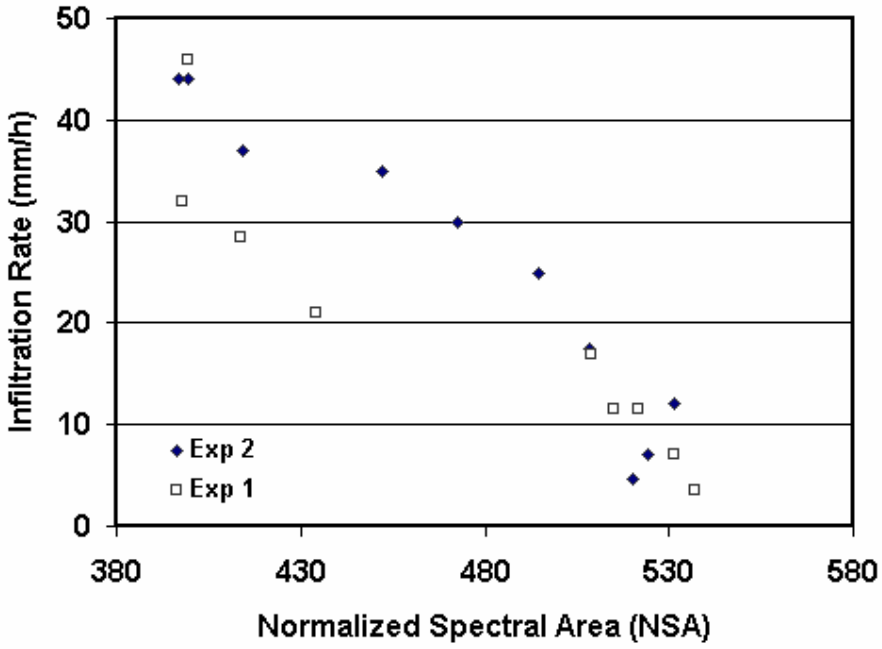

Figure 8: The relationship between the infiltration rate (InR) and the Normalized Spectral Area (NSA) using the laboratory information obtained by the two experiments.

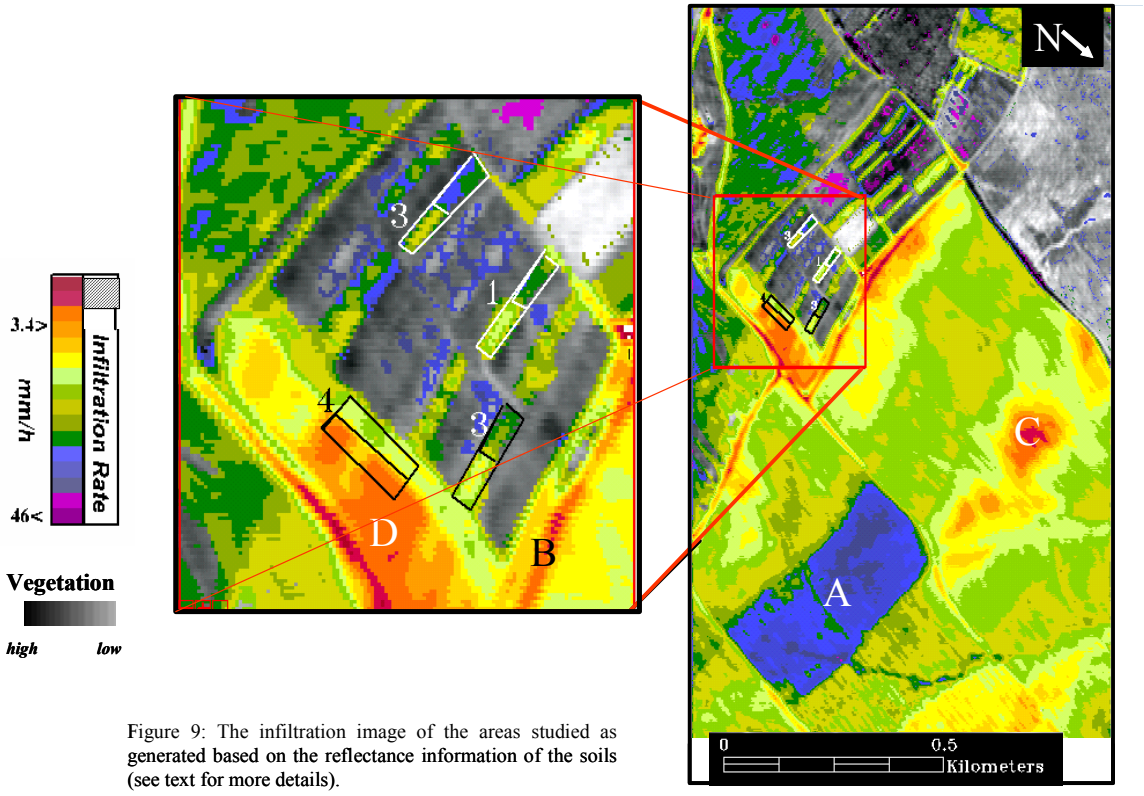

Figure 9: The infiltration image of the areas studied as generated based on the reflectance information of the soils (see text for more details).

SUMMARY AND CONCLUSIONS

The main conclusion of this study is that reflectance properties of Loess crusted soils have a systematic relationship with the crust status. In the soil examined, the albedo parameters across the entire VIS-NIR region hold a significant correlation with raindrop energy, and particularly with infiltration rate. A normalized spectral curve, using a non-crusted soil spectrum as a reference, was suggested to use whereas the area under the ratio curve, suggested to be the parameter for the soil albedo. Doing so enables the utilization of the laboratory spectral relationship with other spectral data sources, such as the hyperspectral sensors introduces. The spectral variation in the field within the selected plots vary within the confident range the laboratory experiment provided. The soils' pixel-by-pixel calculation of the InR shows a reasonable picture for the selected area and their surroundings. We hope that more ideas and thoughts on how to further apply the hyperspectral technology further in this direction will be presented by more other investigators. The AVIRIS sensor in this regard may play an important role as it covers the entire VIS-NIR-SWIR region and has a relatively good signal to noise ratio.

ACKNOWLEDGMENT

This study was conducted under a CIRES fellowship foundation program at Center for the Study of Earth from Space (CSES) University of Colorado at Boulder.

REFERENCES

ACORN, 2001. Atmospheric Correction Now, Analytical Imaging and Geophysics LLC Version 3.12.

Agassi, M., and J. M. Bradford, 1999. "Methodologies for interrill, soil erosion studies." *Soil & Tillage Research* 49: 277–287.

Ben-Dor, E., N. Goldshalager, M. Benyamini, and D. G. Blumberg, 2003. The Spectral Reflectance properties of Soil's structural crust in the SWIR spectral region (1.2–2.5μm), *Soil Science Society of American Journal* 67:289–299.

Dan, Y., and Z. Raz, 1970. *Soil Association Map of Israel.* Volcani Institute for Agriculture Research, Israel (in Hebrew).

Gaffey, S. Y., 1986. "Spectral reflectance of carbonate minerals in the visible and in near infrared (0.35–2.55 μm): calcite, aragonite and dolomite." *American Minerals* 71: 151–162.

Goldshalager, N., E. Ben-Dor, Y. Benyamini, D. Blumberg, and M. Agassi, 2001. "The spectral reflectance of soil's structural crust in the SWIR region 1.2–2.5 μm." *Terra Nova* 7:23–55.

Goldshalager N., E. Ben-Dor, Y. Benyamini, M. Agassi, and D. Blumberg, 2002. Soil Crusting and Infiltration Processes as Monitored by Soil Reflectance Spectroscopy in the SWIR region, *Remote Sensing of Environment Journal (in press).*

Keren, R., and M. J. Singer, 1989. "Effects of low electrolyte concentration on hydraulic conductivity of clay-sand-hydroxypolymer systems," *Soil Science Society of America Journal* 53: 349–355.

Keren, R., and M. J. Singer, 1991. "Hydroxy-aluminum's effects on permeability of clay-sand mixtures," *Soil Science Society of America Journal* 55: 61–65.

Mäkisara, K., M. Meinander, M. Rantasuo, J. Okkonen, M. Aikio, K. Sipola, P. Pylkkö, and B. Braam, 1993. "Airborne imaging spectrometer for applications (AISA)," in *International Geosciences and Remote Sensing Symposium Digest*, (Tokyo, Japan), pp. 479–481.

McIntyre, D. S., 1958. "Permeability measurement of soil crusts formed by raindrop impact," *Soil Science* 85: 185–189.

Morin, J., and Y. Benyamini, 1977. “Rainfall infiltration into bare soil,” *Water Resour. Res*. 13(13): 813–817.
Morin, J., D. Goldberg, and I. Singer, 1967. “Rainfall simulator with rotating disk,” *Trans American Society of Agriculture Engineering* 10: 74–79.
Soil Survey Staff, 1975. *Soil Taxonomy: A Basic System of Soil Classification for Making and Interpreting Soil Surveys*, Handbook, U.S. Dept. Agriculture, 436.